

STUDY OF THE RHEOLOGICAL BEHAVIOUR OF DIFFERENT CERAMIC POWDER MATERIALS

J.L. Amorós, G. Mallol, B. Campos, M.J. Orts, M.C. Bordes

⁽¹⁾ Instituto de Tecnología Cerámica (ITC).
Asociación de Investigación de las Industrias Cerámicas (AICE)
Universitat Jaume I. Castellón. Spain.

ABSTRACT

The study has characterised the rheological behaviour of 20 powder materials used in the manufacture of ceramic tiles, frits, and glazes, with a rotational shear cell. This technique, which is novel for these types of powders, allows their flow curves to be measured. The experimental results were used, applying a model developed by the Instituto de Tecnología Cerámica, to calculate each material's cohesion and flow functions, parameters that characterise a material's flowability.

The study demonstrates the usefulness of this technique for studying powder behaviour during handling, as a methodology for controlling powder flowability and for designing powder-handling facilities. With a view to relating the behaviour of the powder materials to their physical properties, the size and distribution of the powder particles and agglomerates, their real density, and uncompacted powder bed density were measured, while particle shape was characterised by photography with a scanning electron microscope. It has been attempted to relate the differences found in the rheological behaviour of the powders to some of their physical properties, such as compactness, particle and/or agglomerate size, shape, etc.

1. INTRODUCTION

In industrial processes that use materials in the form of solid particulates, also known as granular material or simply powder, in certain process stages, problems tend to occur more frequently than in those that handle fluids^[1,2,3]. The origin of these problems lies in the fact that the flow characteristics of the particulate beds are less well understood and more poorly characterised than those of homogeneous fluid streams^[4].

The manufacturing processes of tiles, frits, and ceramic pigments are not foreign to these problems. In effect, the development of basic operations such as storage, transport, mixing, milling, granulation, proportioning, compaction, fluidisation, etc., present in most ceramic materials production processes, is highly conditioned by powder flowability. However, it may be noted, first, that there is no universally applicable test or index that allows powder flow characteristics or flowability to be determined. On the other hand, the relation of the test should also be based on the objective pursued with the flowability measurement.

The tests most commonly used in characterising powder flowability are those based on the determination of flow curves, measurement of the bulk densities of consolidated particle beds (Hausner ratio, Carr index, etc.), compression tests, measurement of the rest angle, and determination of the flow rate. In this study, the methods based on the determination of the powder flow curves have been used, because they allow determination of the mechanical properties of the beds under different consolidation conditions and provide information for designing equipment used in the handling and storage of powders (silos, hoppers, etc.)

1.1. METHODS OF CHARACTERISING POWDER FLOWABILITY BASED ON THE DETERMINATION OF THE FLOW CURVES. MATERIAL FLOW FUNCTION.

These methods are based on studying the rheological behaviour of powders subjected to normal and shear stresses. For a powder to flow, the applied shear stress needs to be larger than the threshold or yield stress (just as in plastic fluids). However, unlike the latter, the magnitude of the threshold shear stress, τ , or shear strength, depends on the consolidation conditions to which the powder bed has been subjected and the normal stress that acts upon the shear plane when bed flow or rupture (σ) commences. Therefore, the flowability characterisation by these procedures is based on determining, for a given bed compactness (ϕ), the variation of shear strength (τ) with normal stress (σ), known as the flow curve or yield loci according to Jenike^[5].

In order to obtain the flow curves, different types of shear cells are used (uniaxial, biaxial, annular, and rotational, etc.), whose configuration, methodology of use, and comparative advantages and disadvantages have been extensively described in the literature^[6].

The flow curves allow calculation of three types of mechanical strength of the bed: shear or cohesion strength (C), tensile strength (T) and compression strength (f_c). In order to illustrate clearly the concept of compression strength (f_c) a hypothetical compression test, proposed by Jenike in his original work^[5] (Figure 1-a), will be used. Let it be assumed that a powder bed is compacted inside a cylindrical mould with a cross-section A, in which powder friction with the walls is negligible, applying a normal force ($\sigma_1 A$). The consolidated powder is then withdrawn from the mould

and subjected to increasing compression force ($f_c A$) until rupture at a force value ($f_c A$). Repetition of this experiment for different values of σ_1 would yield the pairs of values (σ_1, f_c) , which constitute the flow function of a powder material (MFF), defined by Jenike^[5] as the variation of the compression strength of a powder bed (f_c), free of any stress or envelopment, obtained by compaction at a certain compacting pressure (σ_1), as a function of that compacting pressure. Although this hypothetical experiment illustrates the concept very well, it has no practical usefulness, basically because of the impossibility of eliminating powder/mould friction and of consolidating cylinders with uniform bulk densities, when the cylinders are long.

Shear strength, C , and tensile strength, T , may be illustrated in the same way as above (Figure 1-a). Thus, the values of C and T correspond to the shear stress or tensile strength value, respectively, which need to be applied to break up a powder bed, free of any envelopment or stress, obtained by application of a normal stress σ_1 . To obtain the different types of mechanical strength of the beds, the tensorial calculation^[7,8,9] is applied to the flow curves measured with the shear cells (Figure 1-b).

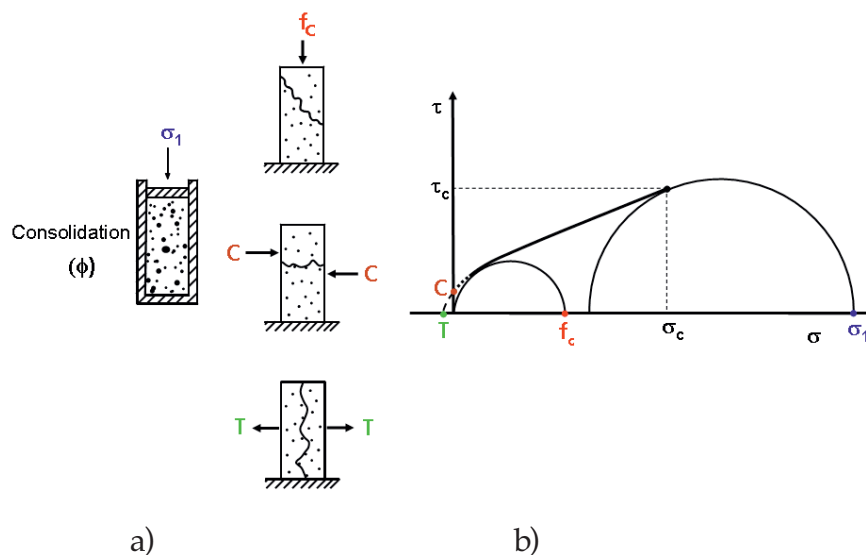


Figure 1. Hypothetical experiment to illustrate the different types of mechanical strength of the bed (a) and calculation of σ_1 , C , T , and f_c from the flow curve (b)

When it comes to ascertaining the rheological behaviour of a powder in a given process (storage, transport, etc.) or to comparing its flowability with that of other particulate materials, it is necessary to specify the maximum normal stress (σ_1) to which the powder will be subjected, since its mechanical properties are a function of that stress. Jenike proposes the quotient σ_1/f_c , used by some researchers as a measure of powder flowability.

Obviously, that ratio depends on bed compactness (ϕ) or on the consolidation stress (σ_1), analogously to what happens with the apparent viscosity of a non-newtonian fluid. As a result, the use of this ratio, commonly termed the flow factor ($ff_c = \sigma_1/f_c$), as a measure of flowability is often incorrect and should only be used for comparative purposes between different powders when the value of σ_1 is fixed. Nevertheless, the flow factor, ff_c , is probably the most widely used index for defining the flowability of particulate materials, since it allows them to be classified as a function of their flowability (Table 1).

ff_c	< 2	2-4	4-10	>10
Behaviour	No flow	Cohesive	Easy flowing	Free flowing

Table 1. Flow behaviour with respect to the flow factor (ff_c) according to Jenike.

1.2. FLOW CURVES OF A POWDER. DESCRIPTIVE EQUATIONS OF THE PHENOMENON

The general shape of the flow curves of particle beds, for any state of consolidation, is very similar and displays the following common characteristics: for high normal stress, σ , values it consists of a practically straight stretch, whereas for small and even negative values of this variable it displays a convex curvature, which becomes more pronounced as the powder becomes more cohesive (Figure 2).

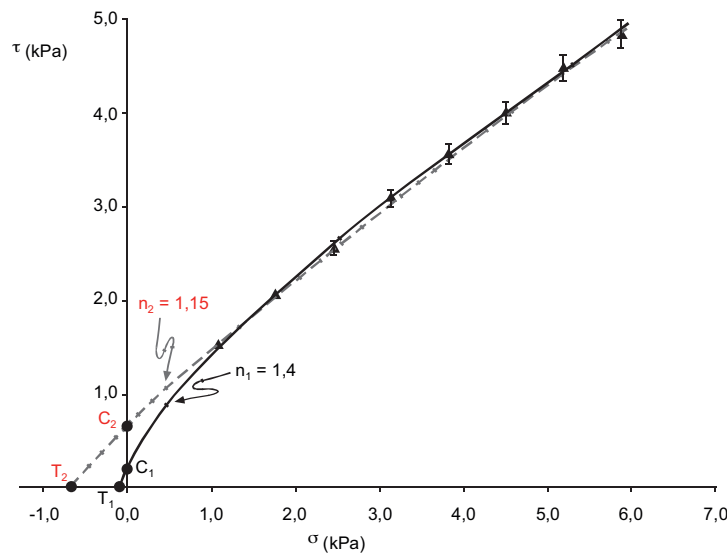


Figure 2. Flow curve of a powder bed. Fit of the experimental values to equation (1), using different values for the parameters.

In 1965 Ashton et al.^[10] proposed equation (1), also termed the Warren-Springs Laboratory (WSLA) equation, in order to describe the flow curve analytically and they tried to justify it by physical arguments based on the attraction and repulsion forces present at the interparticle contact points:

$$(1) \quad \left(\frac{\tau}{C}\right)^n = \frac{\sigma}{T} + 1$$

where n is the shear index.

Although equation (1) is frequently mentioned in the literature, and its authors tried to justify it physically, it has never been used in practical applications (silo design, etc.), nor has the shear index “ n ” been used to characterise powder flowability. This is essentially because of the high uncertainty in the estimation of parameters T , C , and n , which leads to different flow curves for the same experimental values, particularly in the low consolidation stress region (Figure 2).

Even though, as Jenike ^[5] already indicated, the flow curve departs significantly from a straight line for small values of normal stresses, σ , other researchers, either because they omit to work in this stretch of the curve or because they consider that in most cases the departures from linearity are small, fit the experimental results of the yield tests to the Coulomb equation:

$$(2) \quad \tau = C + \mu\sigma$$

where μ is the internal friction coefficient of the powder, related to the internal friction angle, φ_i by means of the relation $\mu = \tan \varphi_i$ ^[8,9].

1.2.1. Proposed model, based on the adhesive contact of elastic spheres (JKR Model)

In 1986 Kendall ^[11] used the model describing the adhesive contact of elastic spheres, originally developed by Johnson, Kendall and Roberts (JKR Model) in 1971 ^[12], to explain the inadequacy of the Coulomb law for quantifying the results of particle bed friction on flat surfaces. However, no study has been found, based on the equation developed by Kendall, or on the JKR model, which develops an equation or model that describes the flow curve of both cohesive and non-cohesive powders.

The model proposed in this study ^[18] is based on the Coulomb fracture criterion. The fracture or yield of the powder in the shear plane on which a total effective normal load, σ^* , acts will occur at a value of τ that meets the yield condition:

$$(3) \quad \frac{\tau}{\sigma^*} \leq \mu = \tan \varphi_i$$

In the Coulomb model, the interparticle surface adhesion force is independent of the external load that is applied; however, in accordance with the JKR model, the interparticle surface adhesion force, F_{ad}^* , and the applied external normal load, W , are mutually related, as has been amply demonstrated experimentally ^[13,14,15], in accordance with the equation:

$$(4) \quad F_{ad}^* = W + 3\gamma\pi R + \left[6\gamma\pi RW + (3\gamma\pi R)^2 \right]^{1/2}$$

where γ is the surface energy of the spheres.

Taking into account that in the powder bed fracture plane there will be a number of contacts per unit apparent surface area, n ; assuming the fracture condition, equation (3); and the definition of cohesion allows the equation of the flow curve to be obtained:

$$(5) \quad \tau = \frac{C}{2} + \sigma\mu + \left(\frac{C}{2} \right)^{1/2} \left[2\sigma\mu + \frac{C}{2} \right]^{1/2}$$

2. OBJECTIVE

The objectives of this study were as follows:

- To verify the validity of the proposed model to describe the flow curves of ceramic powders.

- To characterise the rheological behaviour of different powder materials used in the manufacture of tiles, frits, and ceramic pigments, determining the variation of particle bed cohesion with pressure ($C = f(\sigma_1)$) and the flow function of the material (MFF).
- To study the influence of some physical characteristics of these powders on their rheological behaviour.

3. MATERIALS AND EXPERIMENTAL TECHNIQUES USED

3.1. MATERIALS

In order to carry out this study, 20 particulate materials have been used, grouped in three families.

Family I. This comprised the following powders used in the manufacture of frits and glazes: alumina, barium carbonate, quartz for frits, sodium feldspar, zinc oxide, zirconium silicate for frits, quartz for glazes, and zirconium silicate for glazes.

Family II. This comprised the following particulate materials used in the manufacture of tiles other than porcelain tiles: white clay, red clay, calcium carbonate, dust from bag filters, and spray-dried powder.

Family III. This comprised the following powders used in the manufacture of porcelain tiles: pigment 1, pigment 2, pigment 3, pigment 4, micronised spray-dried powder, and coloured spray-dried powder.

3.2. EXPERIMENTAL TECHNIQUES USED

3.2.1. Determination of particle size distribution by laser diffraction

The particle size distribution of the different powders was determined by dry (vs) and wet (vh) laser diffraction, the difference in the determination being the particle suspending medium: air in the former case, and water in the latter.

The resulting volume distribution was used to determine the parameters d_{50vs} and d_{50vh} , which are the diameters below which there is 50% by volume of the total particles, using air and the water, respectively, as suspending medium.

3.2.2. Particle shape

In order to evaluate particle shape, photographs were taken using a Philips XL30 CP scanning electron microscope (SEM).

3.2.3. Flow curves and compaction diagrams

In order to analyse the densification and flow of the solid particulates subjected simultaneously to normal and shear stresses, a rotational cell like the one schematically illustrated in Figure 3 was used^[16,17]. The experimental procedure followed is the one recommended by the rotational shear cell manufacturer^[16,17], and it allows the

flow curves of the test powders and the compaction diagrams to be rapidly and automatically obtained.

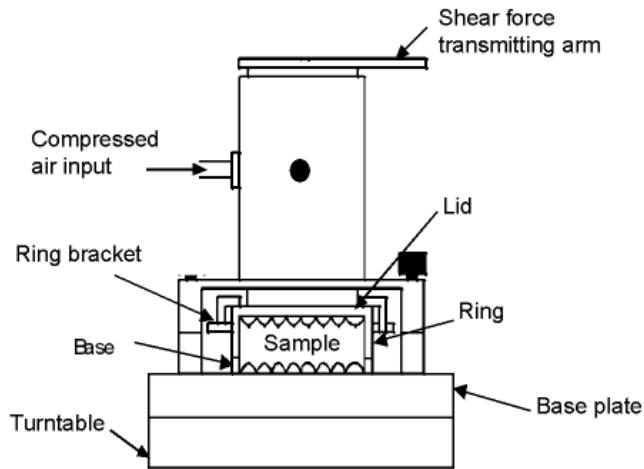


Figure 3. Rotational shear cell.

A study elsewhere^[18] verified the validity of the rotational cell, comparing the flow behaviour of a calcium carbonate powder determined with the rotational cell with that obtained by five European laboratories using Jenike cells, whose results were published in a report by the Directorate-General of Telecommunications, Information Industries, and Innovation of the EC Commission^[19] in 1992.

4. RESULTS AND INTERPRETATION

4.1. VALIDITY OF THE PROPOSED MODEL FOR DESCRIBING THE FLOW CURVES OF THE STUDIED POWDERS

In order to verify the validity of the proposed model, an alumina employed in the manufacture of ceramic frits was used. Figure 4 shows the joint plots of the particle size distributions (PSDs) of the alumina obtained by laser diffraction, using wet and dry sample preparation.

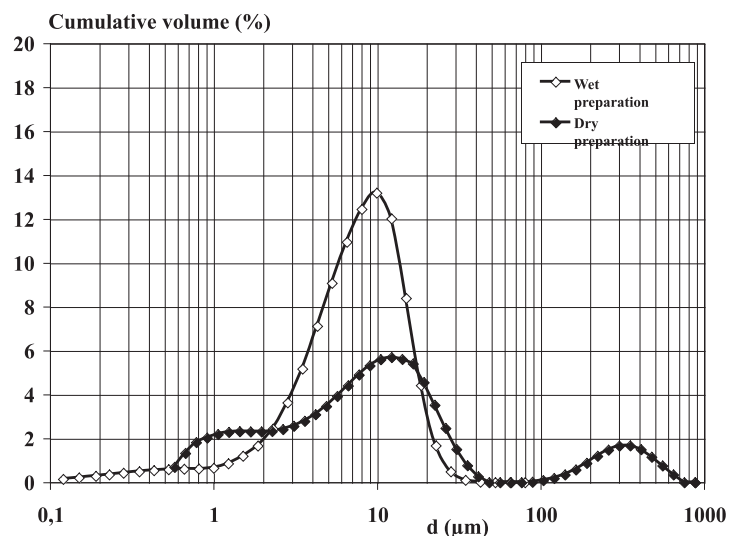


Figure 4. Alumina particle distributions obtained by the wet and dry methods.

Comparison of the two PSDs evidences the material's strong tendency to agglomerate. Thus, though d_{50} is quite similar for both sample preparation procedures (8,36 μm for the sample prepared by the dry method and 8,44 μm for the sample prepared by the wet method), the PSD of the dry sample is much broader, and even displays a second relative maximum around 300 μm , clearly reflecting the presence of particle agglomerates. As will be shown further below, the tendency to agglomerate is especially important in beds made up of fine particles, owing to the greater attraction force and number of interparticle contacts.

The presence of agglomerates in a powder conditions powder rheological behaviour, particularly when the agglomerates have high mechanical strength. Thus, if the particle agglomerates have low mechanical strength, i.e. they are soft, as occurs in most of the particulate materials used as raw materials in frit manufacture, they are readily broken up, affecting the flowability of these powders under low consolidation stresses, the size and nature of the (individualised) primary particle being controlling in most of the consolidation stress range. In contrast, if the agglomerates are hard, as is the case in natural clays and the spray-dried powders used in tile manufacture, the stresses required to break these up will be high, which is why the size of these agglomerates will condition powder flow behaviour.

The alumina described above and the experimental procedure detailed in section 3.2 were used to obtain four flow curves applying 5, 10, 15 and 20 kPa normal stress, σ_c , in bed preparation, respectively. In order to verify the validity of the proposed model for describing the flow curves, the experimental values of the flow curves for the alumina and their fit to equation (5) have been plotted in Figure 5. Very good agreement is observed between the experimental values and the calculated ones (solid lines), no significant deviations being noted between the experimental values and the calculated ones in any stretch of the curve.

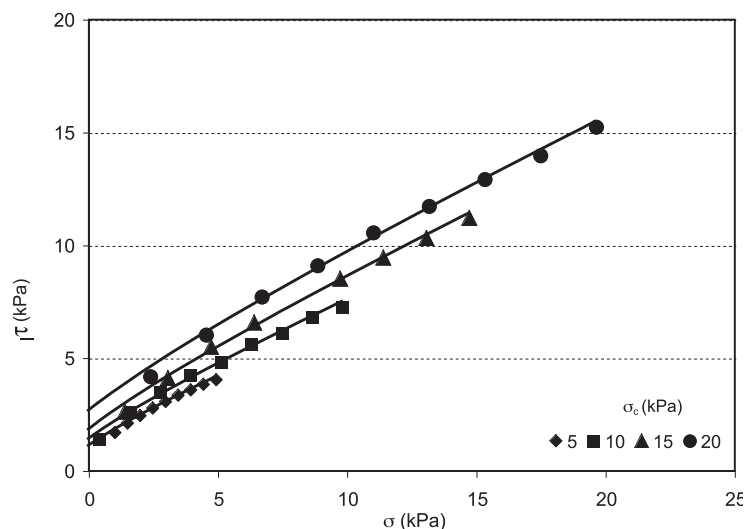


Figure 5. Fit of the experimental values to the proposed model (equation (5)) for the test alumina.

Similar results were found for the other studied particulate materials, corroborating the validity of equation (5) for describing the flow curves.

4.2. INFLUENCE OF CONSOLIDATION STRESS (σ_1) ON BED RHEOLOGICAL BEHAVIOUR

The fit of the experimental values obtained with the shear tests to equation (5) has allowed calculation, for each test powder, of the fitting parameters for the equation (C and μ) and the parameters for consolidation stress, σ_1 , and compression strength, f_c in accordance with the methodology described in the introduction.

The values of compression strength, f_c , cohesion, C , and the friction coefficient, μ , have been plotted as a function of the consolidation stress, σ_1 , for the alumina in Figure 6. It may be observed that when the consolidation stress increases, the three parameters increase. This is because, on the one hand, as σ_1 increases, the particles rearrange to form a more compact packing, displayed on a macroscopic scale by a moderate increase in bed compactness. Parallel to the increase in bed compactness there is an increase in the number of interparticle contacts per unit surface area, which contribute to reducing powder flowability, increasing powder cohesion and bed compression strength.

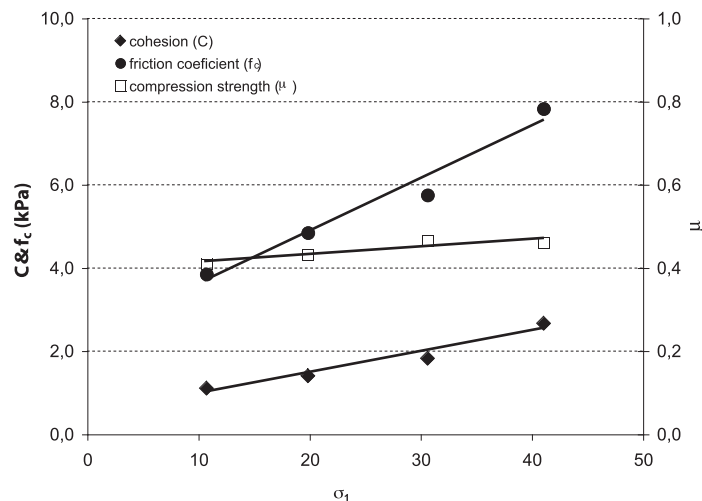


Figure 6. Variation of the alumina rheological parameters, C , μ , and f_c , with consolidation stress, σ_1 .

For the other studied powders the influence of consolidation stress on their rheological behaviour is qualitatively similar to that described for alumina, with the logical differences due to the peculiar physical characteristics of each material, which are set out below.

4.3. INFLUENCE OF THE PHYSICAL PROPERTIES OF THE SOLID PARTICULATES ON POWDER FLOWABILITY

With a view to demonstrating the influence of the physical characteristics of the different powders on their rheological behaviour, it was considered of interest to compare the behaviour of alumina with that of the quartz used in the manufacture of ceramic frits, quartz being a powder with high flowability compared with alumina.

The quartz particle size distributions (PSD) obtained by laser diffraction, with sample preparation by the wet and dry methods respectively, have been jointly plotted

in Figure 7. It shows that this material displays little tendency to agglomerate, since the PSD of the powder prepared by the dry method is similar to that prepared by the wet method, though it is a little broader. In addition, unlike what occurred with the alumina (Figure 4), it is practically monomodal. This behaviour is consistent with the larger average size of the quartz primary particles ($d_{50vh} = 29,1 \mu\text{m}$), compared with that of the alumina ($d_{50vh} = 8,4 \mu\text{m}$), which provide it with a greater agglomeration capacity.

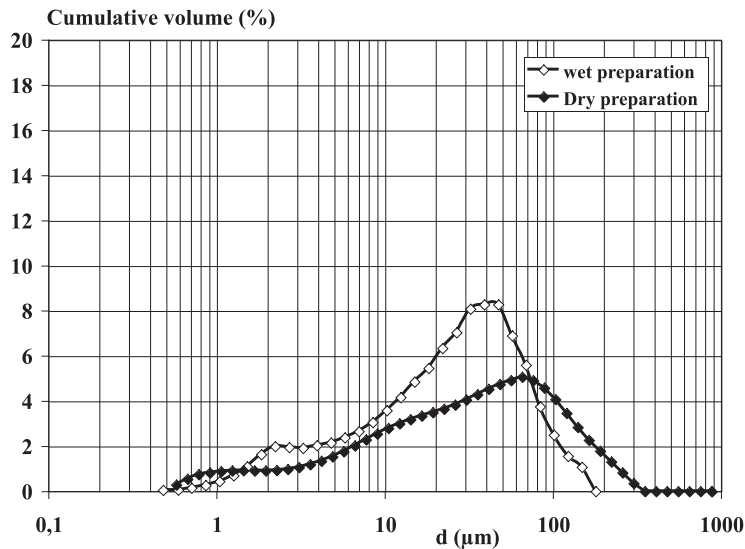


Figure 7. Size distributions of the quartz particles for fusion obtained by the wet and dry methods.

The flow curves of the quartz for fusion obtained by fitting the experimental points to equation (5) have been plotted in Figure 8. As occurred with the alumina (Figure 5), the agreement between the experimental values and the calculated ones (solid lines) is very good; however, unlike the curves corresponding to alumina, those of the quartz display a smaller ordinate at the origin and are much closer, indicating greater flowability and a smaller influence of consolidation stress on the rheological behaviour of the bed.

The flow functions of both particulate materials have been plotted in Figure 9. It shows that, in both cases, when the consolidation stress, σ_1 , increases, compression strength, f_c , rises owing to the effect of σ_1 on bed compactness and on the number of interparticle contacts; however the effect of σ_1 on f_c is much smaller in the quartz particles than in the alumina particles due to the larger size of the quartz particles. If the flow factor of both powders is calculated at a given consolidation stress, for example 20 kPa, ff_{c20} , a value of 4,1 is obtained for the alumina and of 7,1 for the quartz, the behaviour of the alumina being practically cohesive, in accordance with the Jenike classification (Table 1), while the quartz for fusion is easy flowing.

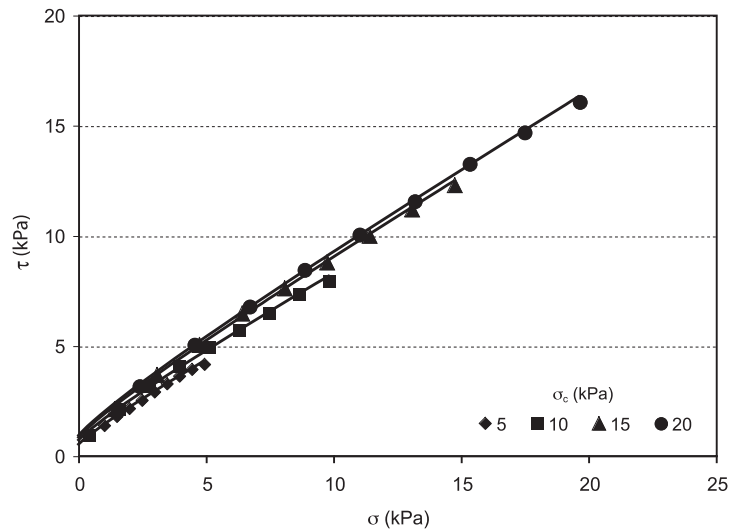


Figure 8. Flow curves corresponding to the quartz for fusion. Fit of the experimental points to equation (5).

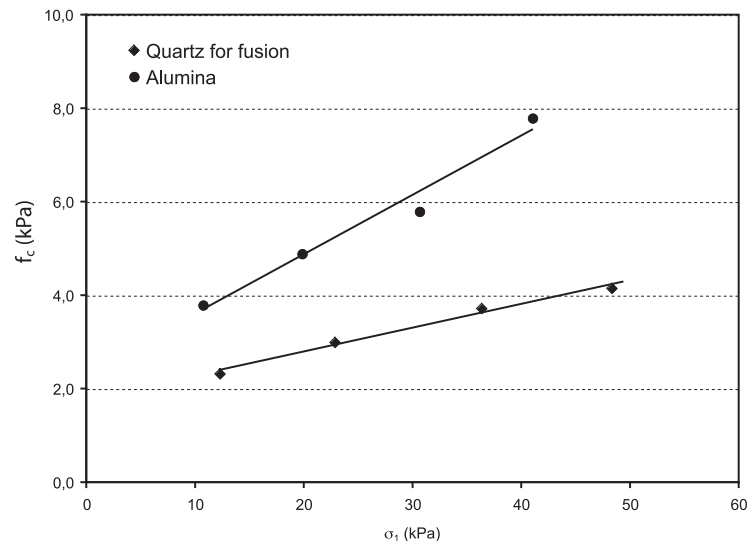


Figure 9. Flow functions of the quartz for fusion and the alumina.

The fact that the behaviour of both particulate materials is directly correlated to the size of their primary particles, measured by the wet method, is because the alumina agglomerates are soft and break up at low consolidation stress values. Once the mechanical strength of the alumina agglomerates (which is low) has been overcome, the rheological behaviour of the bed depends on individual particle size, just as occurred with the quartz across the entire range of consolidation stresses, owing to its low tendency to agglomerate. This behaviour cannot be generalised for all powders since, as set out below, the rheological behaviour of all the analysed particulate materials cannot be fully explained just by the size of the primary particles in the beds.

The flow functions of each material ($f_c = f(\sigma_1)$) were used to calculate the flow factors at 20 kPa (ff_{c20}) for the different test powders. Table 2 presents the results by families, the solid particulates being ordered from lower to higher flowability in

accordance with the Jenike classification (Table 1), taking into account the value of ff_{c20} . The table also shows the d_{50} of each material (d_{50vs} for the dry sample and d_{50vh} for the wet sample), and powder bed compactness at 20 kPa, ϕ_{20} .

Family	Material	ff_{c20}	d_{50vh} (μm)	d_{50vs} (μm)	ϕ_{20}	Behaviour (***)
Frits and Glazes	Zinc oxide	2,1	0,5	9,6	0,120	Cohesive
	Barium carbonate	3,0	2,9	7,7	0,156	Cohesive
	Zirconium silicate for glazes	3,8	1,8	2,7	0,251	Cohesive
	Alumina	4,1	8,4	8,4	0,190	Easy flowing
	Quartz for glazes	4,3	3,4	4,4	0,245	Easy flowing
	Zirconium silicate for fusion	4,5	10,8	15,1	0,251	Easy flowing
	Sodium feldspar	5,0	10,2	17,3	0,345	Easy flowing
	Quartz for fusion	7,1	29,1	30,5	0,405	Easy flowing
Tiles other than porcelain tiles	Kaolin (*)	3,3	10,4	10,8	0,333	Cohesive
	White clay (*)	4,0	6,9	240,2	0,408	Cohesive
	Calcium carbonate	4,3	7,7	7,85	0,355	Easy flowing
	Dust extracted from the press	4,5	10,1	8,76	0,317	Easy flowing
	Red clay (*)	7,0	6,9	248,7	0,463	Easy flowing
	Spray-dried powder	13,3	5,2	306,3	0,402	Free flowing
Porcelain tile	Pigment 1 (**)	2,5	6,9	8,1	0,259	Cohesive
	Micronised spray-dried powder	3,3	5,4	24,3	0,311	Cohesive
	Pigment 2 (**)	3,6	7,8	7,7	0,233	Cohesive
	Pigment 3 (**)	4,7	10,6	9,3	0,265	Easy flowing
	Pigment 4 (**)	5,2	4,7	5,9	0,215	Easy flowing
	Coloured spray-dried powder	10,3	4,8	356,3	0,409	Free flowing

(*) Only particles smaller than 1 mm were characterised (approximately 70% of the total for the three solid particulates), since that is the maximum size recommended by the manufacturer of the rotational shear cell used.

(**) Pigments 1 and 2 are the same pigment, with and without a fluidiser, respectively.

Pigments 3 and 4 are different, and both contain a fluidiser.

(***) According to the classification proposed by Jenike (Table 1)

Table 2. Flow factor at 20 kPa, ff_{c20} , particle size (d_{50vh} and d_{50vs}), and compactness at 20 kPa, ϕ_{20} , of the studied powders.

It may be observed first that, though the value of ff_c reflects the rheological behaviour of the powders quite well, the classification proposed by Jenike from this value is unable to differentiate clearly the behaviour of the analysed particulate materials. In effect, in accordance with this classification, the quartz used in obtaining glazes, which has a very fine particle size ($d_{50vh} = 3,4 \mu\text{m}$), with a small flow factor value ($ff_{c20} = 4,3$), and which usually poses problems in handling, is classified as an easy-flowing powder. This category also includes, according to the Jenike classification,

the quartz for fusion, which has a particle size that is almost 10 times larger, a much larger flow factor ($ff_{c20} = 7,1$), and which poses no problems of flowability in industrial practice.

It may be observed in Table 2 that, for the family of powders used to obtain frits and glazes, in general, when the primary particles size (d_{50vh}) increases, ff_{c20} increases, and the flowability of the solid particulates increases. However, the rheological behaviour of all the powders cannot be explained just by the value of d_{50vh} . Thus, in the case of the red clay and the spray-dried powder, particle primary size is very small (6,9 and 5,2 μm , respectively); yet their flowability is high, as the values of ff_{c20} (7,0 and 13,3, respectively) indicate, since the flow units are large hard agglomerates and not primary particles. The fact is that these particulates are handled in the form of granulates or agglomerates with high mechanical strength, this being much greater than that of the agglomerates that may form in the powders used as raw materials for the manufacture of glazes and frits. Therefore, the rheological behaviour of these particulates will foreseeably be more influenced by the size and shape of the agglomerates than by primary particle size.

When the calculated flow factors for all the powders are plotted jointly as a function of primary particle size, Figure 10, a great scatter is obtained, indicating that powder flowability is not just determined by primary particle size, but that the rheological behaviour of these particulate materials depends on multiple parameters, whose influence on their flowability is moreover complex. These parameters include, in addition to the amplitude of the particle and particle agglomerate size distribution, already noted previously, particle shape, the presence of humidity, or the use of additives (pigments, fluidisers, etc.).

In regard to particle shape, Figure 11 shows the SEM photographs of the quartz used in glaze manufacture, and of the barium carbonate used in frit manufacture. Both powders exhibit practically the same individual particle size ($d_{50vh} = 3,4$ and 2,9 μm , respectively); however, the barium carbonate is cohesive, due to the fibrous and acicular shape of its particles, whereas the quartz is easy flowing owing to the angular, irregular shape of its particles.

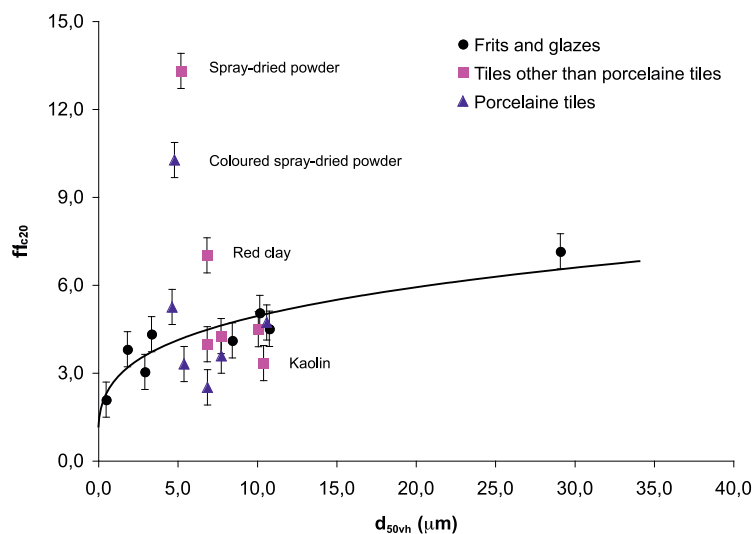


Figure 10. Variation of the flow factor of the studied powders as a function of particle size.

Comparison of the flow factors of the analysed spray-dried powders shows that, though both powders are free flowing, the flow factor of the coloured spray-dried powder ($ff_{c20} = 10,3$) used in porcelain tile manufacture is a little smaller than that of the spray-dried powder used to make other tiles ($ff_{c20} = 13,3$). However, the average size of the primary particles, d_{50vhr} , and of the agglomerates, d_{50vsr} , is very similar. The slight loss of flowability is probably caused by the presence of the pigment in the coloured spray-dried powder. In the case of the pigments, the effect of the fluidiser is noticeable when the flow factors of pigment 1, without a fluidiser, and pigment 2, the same pigment but with a fluidiser, are compared. In this case, the presence of the fluidiser increases the pigment flow factor by 45%.

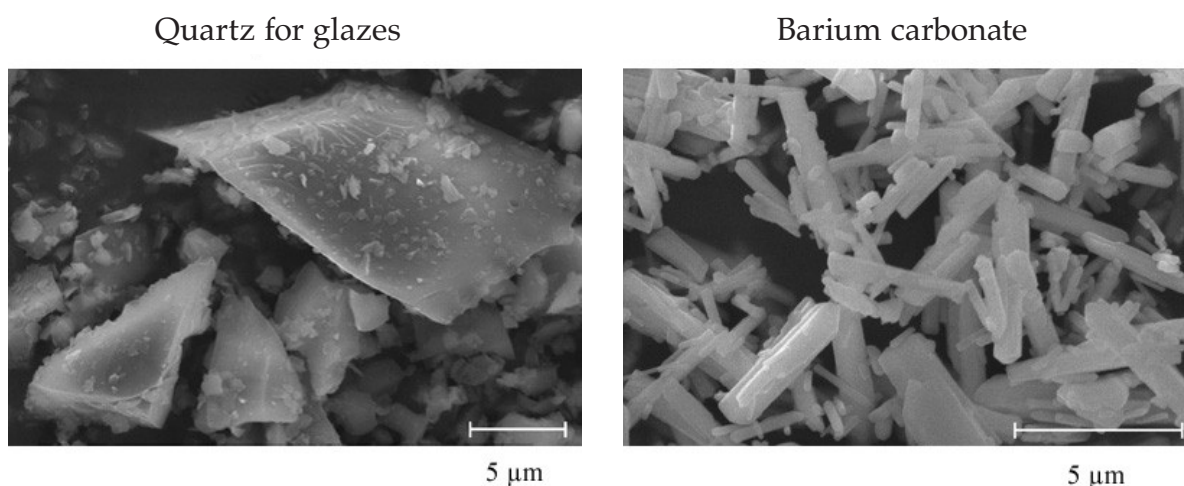


Figure 11. SEM photographs of the quartz for glazes and of the barium carbonate.

5. CONCLUSIONS

The study allows the following conclusions to be drawn:

- The measurement procedure fine-tuned in this study allows quantification of the flowability of particulate materials in different states of consolidation.
- The validity of the proposed model, based on the adhesive contact of elastic spheres, has been verified for describing the flow curves of all the studied materials, solely using the cohesion and the friction coefficient of the powder as parameters.
- Individual particle size is a major parameter in determining the flowability of solid particulates that develop weak particle agglomerates during handling; other parameters that can influence the behaviour of these particulate materials are particle shape and size distribution.
- The rheological behaviour of powders that have strong agglomerates, whose mechanical strength is sufficient to keep them from breaking up under the stresses to which they are subjected during handling, depends on multiple factors and their study is complex.

REFERENCES

- [1] PURUTYAN, H.; PITTENGER, B. H.; CARSON, J. W. Solve solids handling problems by retrofitting. *Chem. Eng. Prog.*, 94(4), 27-39, 1998.
- [2] MARINELLI, J.; CARSON, J.W. Solve solids flow problems in bins, hoppers, and feeders. *Chem. Eng. Prog.*, 88(5), 22- 28, 1992.
- [3] KNOWLTON, T.M. et al. The importance of storage, transfer and collection. *Chem. Eng. Prog.*, 90(4), 44-54, 1994.
- [4] DE JONG, J.A.H.; HOFFMANN, A.C.; FINKERS, H.J. Properly determine powder flowability to maximize plant. *Chem. Eng. Prog.*, 95(4), 25-33, 1999.
- [5] JENIKE, A.W.; JOHANSON, J.R. Review of the principles of flow of bulk solids. *CIM Trans.*, 73, 141-146, 1970.
- [6] SCHWEDES, J. Review on testers for measuring flow properties of bulk solids. *Granular Matter.*, 5, 1-43, 2003.
- [7] SCHULZE, D. Flowability of bulk solids: definition and measuring principles. *Chem. Eng. Technol.*, 67, 60-68, 1995.
- [8] TIMOSHENKO, S.; GOODIER, J. *Teoría de la elasticidad*. 2ª ed. Bilbao: Urmo, 1975.
- [9] WILLIAMS, J.C. The storage and flow of powders. En : RHODES, M.J. (Ed.). *Principles of powder technology*. Chichester: John Wiley, 1990, p. 91-118.
- [10] ASHTON, M.D. et al. Some investigations into the strength and flow properties of powders. *Rheol. Acta*, 4, 206-218, 1965.
- [11] KENDALL, K. Inadequacy of Coulomb's friction law for particle assemblies. *Nature*, 319(16), 203-205, 1986.
- [12] JOHNSON, K.L.; KENDALL, K.; ROBERTS, A.D. Surface energy and the contact of elastic solids. *Proc. Royal Soc. London A*, 324, 301-313, 1971.
- [13] HEIM, L.O. et al. Adhesion and friction forces between spherical micrometer-sized particles. *Phys. Rev. Lett.*, 83(16), 3328-3331, 1999.
- [14] HEIM, L.O. et al. Adhesion force between individual gold and polystyrene particles. *J. Adh. Sci. Technol.*, 16, 829-843, 2002.
- [15] ECKE, S.; BUTT, H.J. Friction between individual microcontacts. *J. Colloid. Interface Sci.*, 244(2), 432-435, 2001.
- [16] PESCHL, I.A.S.Z.; COLIJN, I.H. New rotational shear testing technique. En: *International Powder & Bulk Solids Handling & Processing Conference*. Chicago: Powder Advisory Ctre, 1976, p. 12-21.
- [17] PESCHL, I.A.S.Z. Measurement and evaluation of mechanical properties of powders. *Powder Handling Process.*, 1(2), 135-14, 1989.
- [18] MALLOL GASCH, J.G. *Densificación y flujo de lechos de partículas de cuarzo [Tesis doctoral]*. Castellón: UJI, 2006.
- [19] AKERS, R.J. The certification of a limestone powder for Jenike shear testing: final report. Luxembourg: Office for official publications of the European communities, 1992.